Contemporary Imaging and Reporting Strategies for Head and Neck Cancer: MRI, FDG PET/MRI, NI-RADS, and Carcinoma of Unknown Primary—*AJR* Expert Panel Narrative Review

Sugoto Mukherjee, MD[1], Nancy J. Fischbein, MD[2], Kristen L. Baugnon, MD[3], Bruno A. Policeni, MD[4], Prashant Raghavan, MD[5]

Neuroradiology/Head and Neck Imaging · *AJR* Expert Panel Narrative Review

Keywords

head and neck squamous cell carcinoma, MRI, neck carcinoma of unknown primary, Neck Imaging Reporting and Data System, PET/MRI

Submitted: Jun 10, 2022
Revision requested: Jun 22, 2022
Revision received: Aug 8, 2022
Accepted: Aug 29, 2022
First published online: Sep 7, 2022
Version of record: Nov 23, 2022

The authors declare that there are no disclosures relevant to the subject matter of this article.

CT, MRI, and FDG PET/CT play major roles in the diagnosis, staging, treatment planning, and surveillance of head and neck cancers. Nonetheless, an evolving understanding of head and neck cancer pathogenesis, advances in imaging techniques, changing treatment regimens, and a lack of standardized guidelines have led to areas of uncertainty in the imaging of head and neck cancer. This narrative review aims to address four issues in the contemporary imaging of head and neck cancer. The first issue relates to the standard and advanced sequences that should be included in MRI protocols for head and neck cancer imaging. The second issue relates to approaches to surveillance imaging after treatment of head and neck cancer, including the choice of imaging modality, the frequency of surveillance imaging, and the role of standardized reporting through the Neck Imaging Reporting and Data System. The third issue relates to the role of imaging in the setting of neck carcinoma of unknown primary. The fourth issue relates to the role of simultaneous PET/MRI in head and neck cancer evaluation. The authors of this review provide consensus opinions for each issue.

The incidence of smoking-related oral cavity, laryngeal, and pharyngeal cancers in the United States has decreased over the past 2 decades, offset by an increasing incidence of human papillomavirus (HPV)-associated oropharyngeal cancers. Unlike non–HPV-associated head and neck squamous cell carcinoma (HNSCC), HPV-associated HNSCC occurs in young patients, is located predominantly in the oropharynx, frequently presents as an asymptomatic neck mass, and has better prognosis [1]. An evolving understanding of underlying oncogenic pathways in HPV-associated HNSCC has led to increased emphasis on molecular staging using expression of the tumor suppression gene *p16* as a surrogate marker for HPV status. Advances in surgical techniques, radiotherapy, and targeted chemotherapy and immunotherapy regimens have led to improved patient survival [2] and increased reliance on imaging for diagnosis, staging, and surveillance. Imaging currently plays a central role in patient management. Nonetheless, numerous areas of uncertainty remain in the imaging of head and neck cancer, including selection of the optimal modality, the role of advanced imaging techniques, and the approach to surveillance imaging. In this review, we address issues related to MRI technique, surveillance imaging, imaging of neck carcinoma of unknown primary (NCUP), and the role of PET/MRI in the imaging of head and neck cancer.

What Are the Minimum Requirements for an MRI Protocol for Assessing Head and Neck Cancer, and What Additional Sequences Should Be Considered?

CT and MRI are complementary for the evaluation of head and neck cancer, with each potentially providing unique information that may impact management. Compared with CT, MRI offers superior soft-tissue contrast and bone marrow assessment as well as the possibility for functional evaluation. Given the range of possible sequences, MRI protocols may be tailored to address the specific clinical question [3]. In this section, we review the routine standard and optional advanced MRI sequences used to evaluate the patient with head and neck cancer.

ARRS is accredited by the Accreditation Council for Continuing Medical Education (ACCME) to provide continuing medical education activities for physicians.

The ARRS designates this journal-based CME activity for a maximum of 1.00 AMA PRA Category 1 Credit™. Physicians should claim only the credit commensurate with the extent of their participation in the activity.

To access the article for credit, follow the prompts associated with the online version of this article.

doi.org/10.2214/AJR.22.28120

AJR 2023; 220:160–172

ISSN-L 0361–803X/23/2202–160

[1]Department of Radiology and Medical Imaging, University of Virginia Health System, PO Box 800170, 1215 Lee St, Charlottesville, VA 22908-1070. Address correspondence to S. Mukherjee (sm5qd@virginia.edu).

[2]Department of Radiology, Stanford University, Palo Alto, CA.

[3]Department of Radiology and Imaging Services, Emory University School of Medicine, Atlanta, GA.

[4]Department of Radiology, University of Iowa School of Medicine, Iowa City, IA.

[5]Department of Diagnostic Radiology and Nuclear Medicine, University of Maryland School of Medicine, Baltimore, MD.

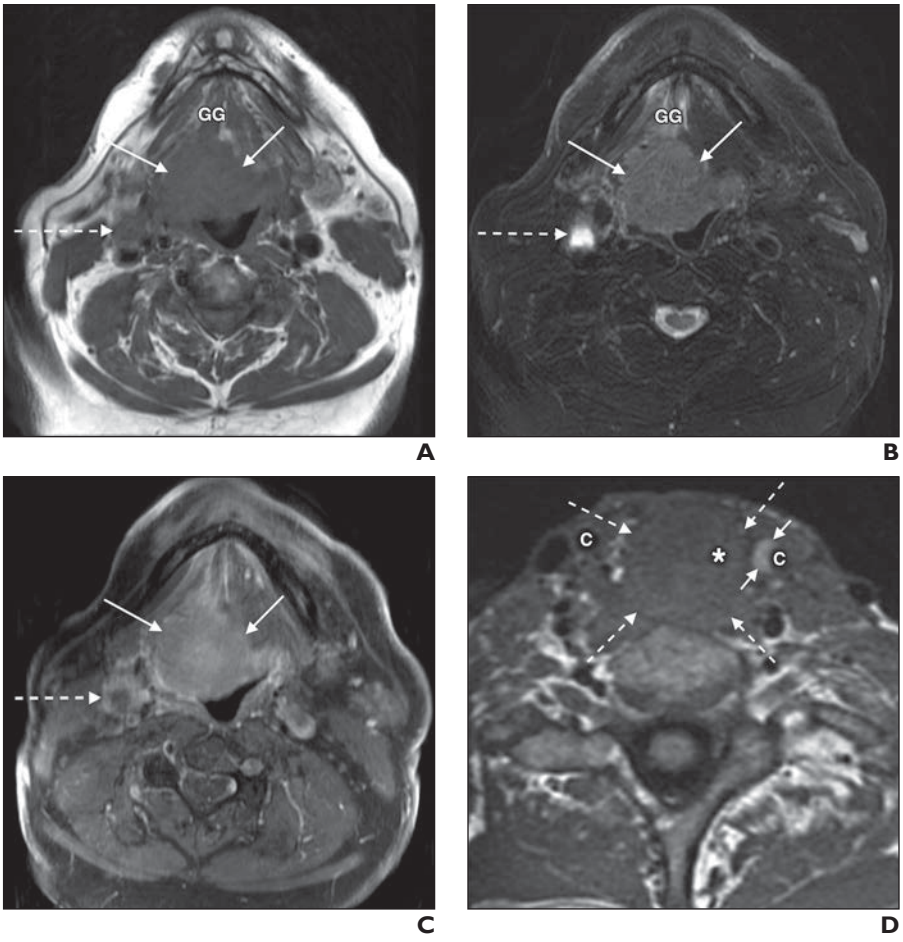

Fig. 1—Standard head and neck MRI sequences.
A–C, 69-year-old man with odynophagia and hemoptysis. Axial T1-weighted image (5-mm thickness) (**A**) shows large oropharyngeal soft-tissue mass (*solid arrows*) infiltrating fat planes and muscle at base of tongue and floor of mouth. Mass was diagnosed as *p16*-negative squamous cell carcinoma of base of tongue and was categorized as T4a given infiltration of genioglossus (GG) muscle. Enlarged metastatic right level 2A lymph node is also present (*dashed arrow*). Axial T2-weighted image with fat suppression (**B**) shows intermediate signal intensity of mass (*solid arrows*), differentiating it from hypointense muscle and suppressed fat. Image also shows peritumoral edema of anterior floor of mouth and GG muscle as well as marked hyperintensity of metastatic right level 2A lymph node (*dashed arrow*), consistent with central necrosis. Axial contrast-enhanced T1-weighted image with fat suppression (**C**) shows moderate diffuse enhancement of mass (*solid arrows*). Right level 2A lymph node (*dashed arrow*) shows irregular peripheral enhancement, consistent with central necrosis.
D, 66-year-old man with recurrent squamous cell carcinoma after laryngectomy. Axial T1-weighted image (two-slice thickness), reconstructed from sagittal 3D acquisition (CUBE, GE Healthcare), shows large soft-tissue mass involving neopharynx and surgical bed (*dashed arrows*), traversed by nasogastric tube (*asterisk*). Patient had experienced recent left cerebral hemisphere ischemic infarction. Sequence has black-blood characteristics, and both common carotid (denoted by C) lumens are well visualized. Left common carotid artery shows intramural hematoma (*solid arrows*), consistent with hemorrhage into atherosclerotic plaque.

Standard MRI Sequences

Noncontrast T1-weighted imaging—Noncontrast T1-weighted images depict head and neck anatomy (Fig. 1A), showing the integrity of fat planes between structures. The status of fat planes adjacent to primary tumors and lymph nodes provides information about tumor margins and extension. T1-weighted images also help assess tumor infiltration into bone, on the basis of disruption of the normal fat signal intensity of bone marrow in adult patients. Marrow infiltration may result in upstaging. For example, in patients with nasopharyngeal carcinoma, MRI evidence of marrow infiltration at the skull base changes the tumor category from T1 or T2 to T3. Unless used to evaluate an intrinsically T1-hyperintense lesion, precontrast T1-weighted images should not be acquired with fat suppression (FS), which results in similar signal intensity of fat, muscle, and tumor and consequent poor contrast resolution.

T1-weighted images should be reviewed in two or three planes [4]. The axial T1-weighted image is the workhorse sequence of head and neck cancer MRI protocols, providing a general anatomic overview and highlighting anatomic distortions and asymmetries that may be critical for localizing and characterizing tumor. Sagittal T1-weighted images help assess midline structures such as the clivus and cervical spine and are also well suited for evaluation of the nasopharynx, base of the tongue, and posterior pharynx. Coronal T1-weighted images offer excellent visualization of the orbits, sinonasal cavity, and skull base foramina, with the latter commonly involved by perineural tumor extension. Axial, sagittal, and coronal T1-weighted images may be obtained as individual 2D acquisitions or as reconstructions from a single 3D acquisition. Three-dimensional acquisition performed using a spin-echo method offers time savings, thinner slices, and black-blood images that may aide assessment for vessel compromise [5] (Fig. 1D).

T2-weighted imaging—T2-weighted images are typically acquired with FS to increase the contrast between generally hyperintense tumor or lymphoid tissue versus a hypointense background of muscle and suppressed fat [6] (Fig. 1B). FS is commonly achieved using Dixon-type methods or STIR [7]. FS may be inhomogeneous in areas of magnetic field inhomogeneity (e.g., from dental amalgam, surgical clips, ferromagnetic implants, spinal fusion constructs, or air-bone interfaces), leading to image artifacts. In such situations, acquisition of T2-weighted images without FS may be considered.

On T2-weighted images with FS, primary tumors typically are mildly hyperintense to head and neck soft tissues. Hence, this sequence is critical for tumor identification and assessment of the size, extent, and infiltration of adjacent structures. T2-weighted images also aid in tumor characterization, as squamous cell carcinoma (SCC) is typically intermediate in signal intensity on T2-weighted images, whereas chordomas and chondrosarcomas are typically markedly hyperintense and lymphoma is hypointense on T2-weighted images. Neck lymph nodes are readily

TABLE 1: Representative 2D Head and Neck MRI Protocol

Sequence	Two-Dimensional Imaging			DWI[a]
	T1-Weighted Without FS	T2-Weighted With FS	Contrast-Enhanced T1-Weighted With FS	
No. of imaging plane(s)	≥ 2	≥ 2	≥ 2	1 (Axial)
Slice thickness (mm)	5	5	5	5
Interslice gap (mm)	0–1	0–1	0–1	0–1
No. of slices	40	40	40	40
FOV (cm)	20	20	20	20–24
Matrix	≥ 320 × 224	≥ 320 × 224	≥ 320 × 192	≥ 128 × 128
TR/TE	500/11	7000/110	500/11	3000/80

Note—All sequences are obtained with head, neck, and spine coil or with neck and chest coil. Coil selection is vendor dependent, but for all sequences coil must provide coverage from skull base to thoracic inlet with high SNR. FS = fat suppression.
[a]Performed with echo-planar imaging method and b values of 500–800 s/mm^2.

identifiable on T2-weighted images with FS in comparison with hypointense muscle and suppressed fat. T2-weighted images also show cystic and necrotic change associated with metastatic cervical lymph nodes. At the skull base, T2-weighted images help assess fluid-filled structures such as the Meckel cave for replacement by tumor. In the paranasal sinuses, tumors show intermediate signal intensity on T2-weighted images, allowing differentiation from edematous mucosa and secretions. After treatment, T2-weighted images help assess radiation-related edema and detect persistent or recurrent disease. As recurrence typically shows signal intensity similar to that of the primary tumor, and as the most common head and neck cancers are intermediate in signal intensity on T2-weighted images, T2-weighted imaging with FS facilitates the differentiation of recurrence from a hyperintense posttreatment change. As with T1-weighted images, T2-weighted images may be obtained by multiplanar 2D acquisitions (guided by the disease site and clinical question) or by a 3D T2-weighted image acquisition [5]. However, FS has variable compatibility with 3D methods.

Contrast-enhanced T1-weighted imaging—Contrast-enhanced T1-weighted images of the head and neck are typically obtained with FS so that T1-hyperintense–enhancing tumor may be differentiated from T1-hyperintense fat [6] (Fig. 1C). Gadolinium-based contrast agents (GBCAs) are useful for characterizing lesions on the basis of the presence, degree, and pattern of enhancement and increased sensitivity to intracranial extension of disease. GBCA administration is especially useful for cancers involving sites in proximity to the intracranial compartment, such as the nasopharynx, sinonasal cavity, orbit, and temporal bone. In such cases, the meninges, cisternal segments of cranial nerves, and brain must be scrutinized for involvement.

As with T2-weighted imaging, the addition of FS to contrast-enhanced T1-weighted imaging may introduce inhomogeneity and artifacts in areas of magnetic field inhomogeneities. Artifacts from failed FS can obscure or falsely suggest the presence of pathology, and postcontrast T1-weighted images without FS may be considered in such cases. GBCA administration can also introduce flow-related and pulsation artifacts, which may be mitigated through the use of separate black-blood sequences. Contrast-enhanced T1-weighted imaging with FS has historically been performed as separate 2D acquisitions in the axial and coronal planes, with possible sagittal acquisition performed to assess midline structures. Nonetheless, 3D postcontrast T1-weighted imaging of the head and neck also is now widely performed. The potential disadvantages of the 3D approach include less homogeneous FS and increased motion artifact from longer acquisition times [5].

Recommendation regarding standard sequences—An MRI protocol for the evaluation of a patient with head and neck cancer should include precontrast T1-weighted images, T2-weighted images with FS, and postcontrast T1-weighted images with FS, all reviewed in two or three planes (Table 1). The sequences should provide anatomic coverage from the skull base to the thoracic inlet to fully assess the neck for metastatic lymphadenopathy. Precontrast T1-weighted imaging should not use FS. Although most head and neck imaging is still performed with 2D acquisitions, the increasing availability of 3D sequences optimized for head and neck imaging offers potential benefits in terms of thinner slices, higher spatial resolution, total time savings, and improved vascular evaluation (Table 2). Challenges of 3D techniques include variable availability, potentially impaired FS quality, and motion susceptibility from longer acquisitions.

Optional Advanced MRI Sequences

DWI—DWI is useful in head and neck cancer imaging for characterizing lesion cellularity, thereby informing diagnosis and tumor characterization. DWI also helps evaluate for recurrent disease, as cellular tumor is more likely than posttreatment edema or necrotic tissue to restrict diffusion [8, 9]. Primary or nodal tumor overlooked on conventional sequences may show increased conspicuity on DWI given typical hypointensity of background soft tissue on DWI. DWI has a typical acquisition time of approximately 1–2 minutes, which may aid tumor visualization if other sequences with longer acquisition times are degraded by motion (Figs. 2A and 2B).

Quantitative values derived from ADC maps may also be useful [10]. Although considerable literature has evaluated ADC values of various head and neck pathologies, ADC values overlap among pathologies, and clinical radiology reports typically do not report ADC values. The ADC may nonetheless be assessed qualitatively, a marked reduction is associated with highly cellular entities such as small round blue cell tumors, an intermediate

TABLE 2: Representative 3D Head and Neck MRI Protocol

Sequence	Three-Dimensional Imaging			DWI[a]
	T1-Weighted Without FS	T2-Weighted With FS	Contrast-Enhanced T1-Weighted With FS	
Imaging plane	Sagittal	Sagittal	Sagittal	Axial
Slice thickness (mm)	0.8–1.0	0.8–1.0	0.8–1.0	5.0
Reformatted sequence (mm)	2–5	2–5	2–5	
Slice gap (mm)	≤ 0	≤ 0	≤ 0	0–1
No. of slices	Variable	Variable	Variable	40
FOV (cm)	25	25	25	20–24
Matrix	≥ 256 × 256	≥ 256 × 256	≥ 256 × 256	≥ 128 × 128
TR/TE	690/24	2500/195	600/10	3000/80

Note—Coverage for all sequences is from skull base to thoracic inlet. Three-dimensional sequences provide isotropic data and may be reformatted in any plane. Names of 3D sequences vary among vendors and include CUBE (GE Healthcare), SPACE (Siemens Healthineers), volume isotropic turbo spin-echo acquisition (VISTA, Philips Healthcare), and VIBE. Parameters provided in table are for the CUBE sequence. All sequences are performed with head, neck, and spine coil or with neck and chest coil. Coil selection is vendor dependent, but coil must provide for all sequences coverage from skull base to thoracic inlet with high SNR. FS = fat suppression.
[a]Performed with echo-planar imaging method and high b values of 500–800 s/mm^2.

reduction is associated with SCC or nasopharyngeal carcinoma (Fig. 2C), and no significant reduction is associated with chondrosarcoma (among other entities) [11].

DWI may be technically limited in the head and neck due to air, bone, and soft-tissue interfaces that distort the magnetic field. These distortions are amplified by the use of routine echo-planar imaging (EPI) acquisitions and can be mitigated by the use of non-EPI techniques such as PROPELLER (GE Healthcare) or HASTE (Siemens Healthineers) [12]. However, the non-EPI techniques typically have longer acquisition times that may be considered too time-consuming for imaging the entire neck.

Contrast-enhanced perfusion imaging—Malignant tumors are generally hypervascular compared with normal adjacent tissues, and perfusion information may help predict and monitor treatment response as well as aid posttreatment surveillance [8, 13, 14]. Dynamic contrast-enhanced (DCE) perfusion imaging using GBCA has been applied to differentiate SCC from lymphoma as well as to differentiate hypovascular tumors (e.g., schwannomas) from hypervascular tumors (e.g., paraganglioma) [8, 14]. DCE and dynamic susceptibility contrast (DSC) perfusion imaging (also performed using GBCA) allow determination of perfusion parameters including permeability, blood flow, and blood volume as well as wash-in and washout characteristics based on curves of time versus signal intensity. Perfusion maps facilitate qualitative interpretation of perfusion data [13, 15, 16] (Figs. 2D–2F). Data postprocessing for GBCA-based perfusion imaging may be automated or may require physician or technologist oversight. Artificial intelligence algorithms may facilitate GBCA-based perfusion imaging of the head and neck, providing automated postprocessing pipelines as well as initial assignment of quantitative parameters (e.g., for differentiating tumor from treatment-related change) [17].

Arterial spin labeling perfusion imaging—Arterial spin labeling (ASL) perfusion imaging is based on radiofrequency tagging of protons in flowing blood in the neck. These tagged spins travel to where the flowing blood travels, and by subtracting untagged from tagged images, a tissue perfusion map is created [18, 19]. For routine ASL, a plane in the upper neck is tagged, and the imaging volume extends from the C1–C2 level to the vertex, thereby including the nasal cavity, paranasal sinuses, orbits, and skull base. Assessment of perfusion characteristics of lesions in these locations and of perfusion changes after treatment can help establish a diagnosis and evaluate treatment response. Head and neck cancers are typically well visualized using ASL perfusion imaging given that the tumors are usually at least moderately hypervascular and the background head and neck tissue is hypointense [18] (Figs. 2G and 2H). ASL perfusion imaging has relatively limited application to aerodigestive tract cancers, which are not reliably included in the standard anatomic coverage of the sequence. However, ongoing technical advances may facilitate the greater anatomic coverage and thereby wide applicability of ASL [19].

Recommendation regarding optional advanced sequences—DWI is a rapid and straightforward sequence that can be added to head and neck protocols and does not require additional postprocessing. Given the utility of DWI in assessing primary and nodal disease at the time of diagnosis and during follow-up, as well as in differentiating tumor from other pathologies, its routine use is recommended. Gadolinium-based perfusion imaging is limited not only by various technical challenges as well as the need for postprocessing but also by a lack of consensus regarding selection of clinically relevant parameters derived from DCE and DSC acquisitions. Its routine use therefore is not recommended. Given that ASL perfusion imaging does not require GBCA injection or postprocessing, and given that early clinical experience suggests utility in tumor identification, characterization, and posttreatment follow-up, its use in head and neck cancer protocols should be considered at centers with access to the technique.

How Should Imaging Surveillance Be Managed in Patients With HNSCC?

HNSCC most commonly recurs in the first 3 years after treatment, providing a critical early period for clinical and imaging surveillance [20]. Although groups have attempted to create guidelines based on the available literature, surveillance recommendations vary substantially, and universally accepted

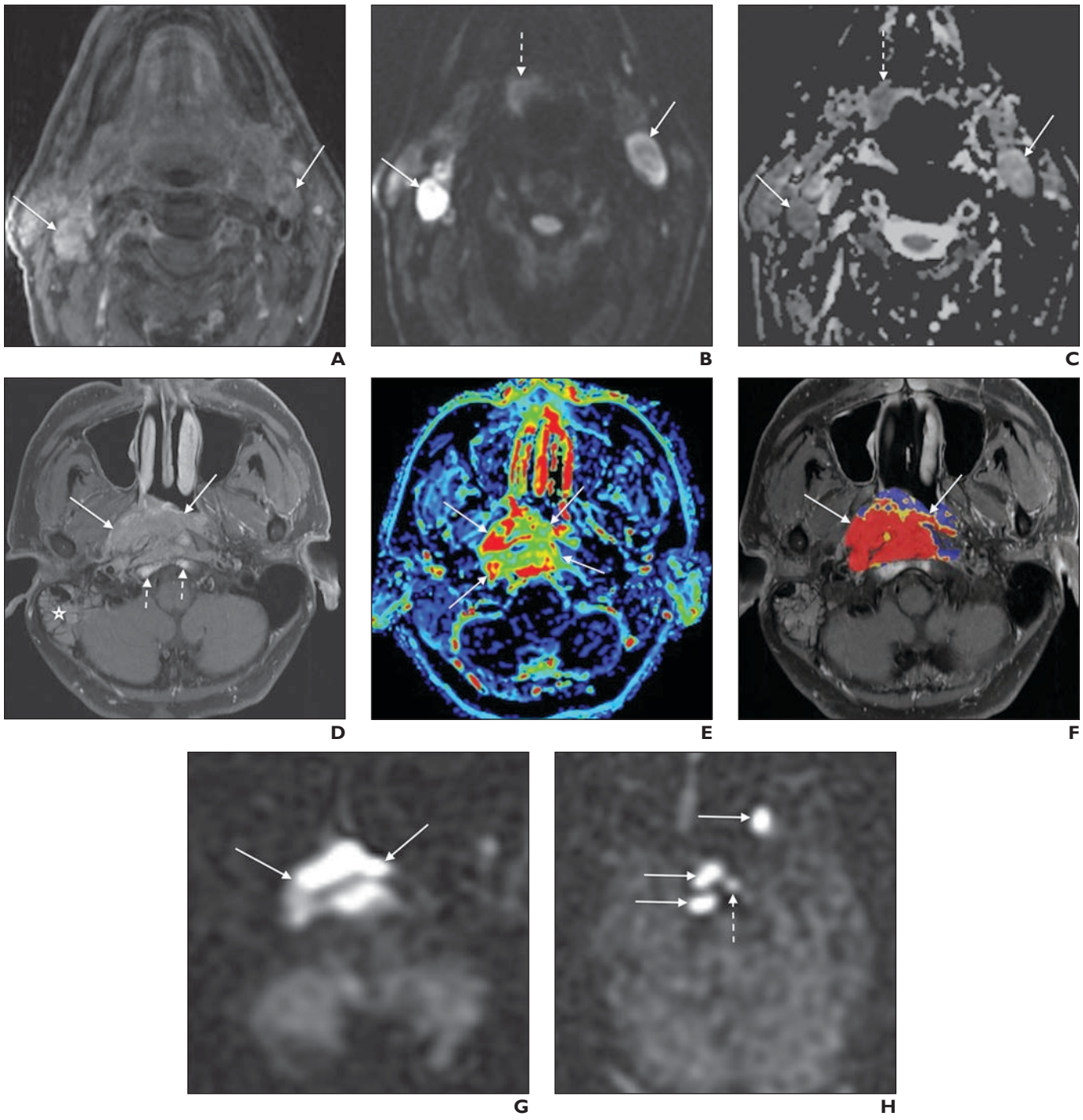

Fig. 2—Advanced head and neck MRI sequences.
A–**C,** 73-year-old man with cervical lymphadenopathy. Axial contrast-enhanced T1-weighted image with fat suppression (**A**) shows bilateral enlarged level 2 lymph nodes (*arrows*). Fine-needle aspiration sample from one of these lymph nodes was consistent with metastasis from *p16*-positive squamous cell carcinoma. Image is degraded by motion, and primary tumor is not clearly identified. Axial DWI (**B**) shows bilateral enlarged level 2 lymph nodes (*solid arrows*) and primary site at right base of tongue (*dashed arrow*). Visualization of primary tumor is facilitated by hypointensity of background tissue on DWI. Motion artifact may also be reduced on DWI given short acquisition times relative to standard sequences. ADC map (**C**) shows hypointensity of bilateral enlarged level 2 lymph nodes (*solid arrows*) and primary site at right base of tongue (*dashed arrow*). Low ADC indicates restricted diffusion, attributable to increased cellularity.
D–**G,** 37-year-old man with aural fullness and newly diagnosed nasopharyngeal carcinoma. Axial contrast-enhanced T1-weighted image with fat suppression (**D**) shows right mastoid effusion (*star*). Large nasopharyngeal mass (*solid arrows*) extends into right parapharyngeal space, prevertebral musculature, and adjacent skull base (*dashed arrows*). Permeability map from dynamic contrast-enhanced perfusion imaging sequence (**E**) shows nasopharyngeal mass (*arrows*) with increased permeability compared with adjacent soft tissue. Tissue blood volume map from dynamic susceptibility contrast perfusion image (**F**), overlaid on axial contrast-enhanced fat-suppressed T1-weighted image, shows red coloration (*arrows*) indicating high blood volume of nasopharyngeal mass. Arterial spin labeling (ASL) perfusion image (**G**) shows marked hyperperfusion of nasopharyngeal mass (*arrows*). ASL perfusion imaging is performed without administration of gadolinium-based contrast material.
H, 68-year-old man who was previously treated for esthesioneuroblastoma. ASL perfusion image shows multiple hyperperfusing foci (*solid arrows*) in right cavernous sinus and left orbit, which were difficult to see on conventional sequences (not shown) without cross-referencing ASL images. Tissue sampling of left orbital focus confirmed recurrent disease, and chemotherapy was restarted. Dashed arrow indicates normal pituitary gland.

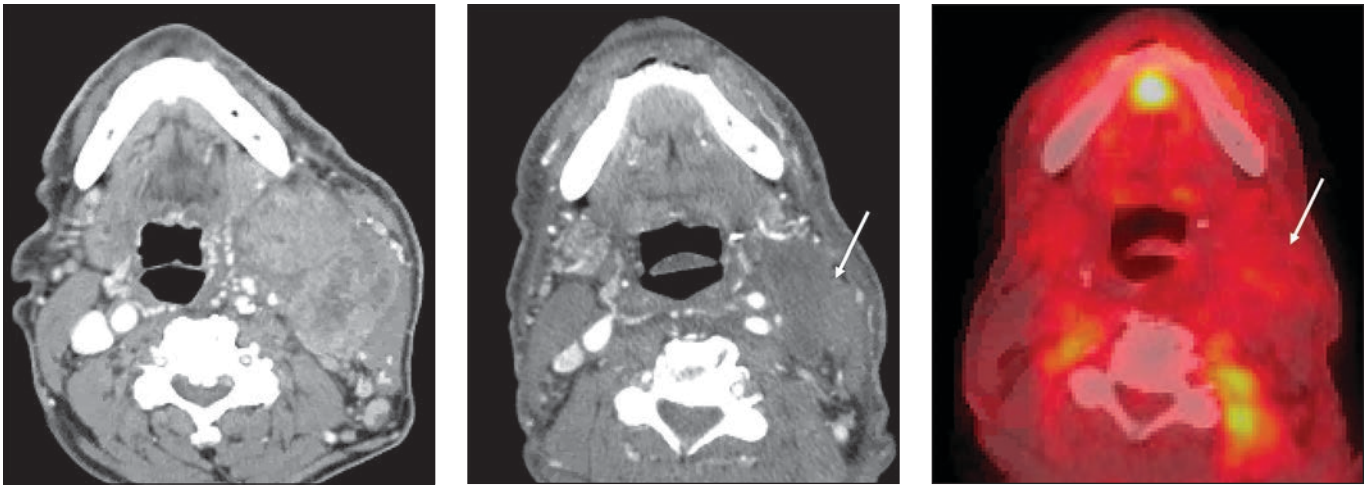

Fig. 3—52-year-old man with history of human papillomavirus–positive squamous cell carcinoma of left tonsil.
A–C, Axial contrast-enhanced image from initial staging CT (**A**) shows metastatic nodal mass in left neck. Axial contrast-enhanced CT image from baseline posttreatment FDG PET/CT (**B**), performed 12 weeks after completion of chemoradiation, shows residual left neck nodal soft tissue (*arrow*). Corresponding axial PET image (**C**) shows absence of FDG uptake by left neck nodal mass (*arrow*). PET/CT examination is consistent with Neck Imaging Reporting and Data System category 1 findings in neck (no evidence of recurrence; routine surveillance recommended).

evidence-based algorithms for the timing and modality of imaging surveillance are lacking. Nonetheless, there is overall agreement that a baseline posttreatment imaging examination should be obtained within 6 months after completion of therapy [21].

The strongest justification for baseline posttreatment surveillance imaging arose from the PET-NECK randomized controlled trial published in 2016 [22]. This study randomized patients who had advanced nodal disease and were receiving concomitant chemoradiation therapy to undergo either planned surgical neck dissection after therapy or PET/CT at 12 weeks after treatment. Patients who underwent baseline posttreatment PET/CT had significantly lower rates of neck dissection, surgical complications, and adverse effects, although they also had similar survival rates, with a cost savings of $2190 per patient [22]. PET combined with contrast-enhanced CT has been shown to be superior to contrast-enhanced CT alone for baseline posttreatment imaging [23, 24]. Absence of FDG uptake in residual soft tissue at the site of regressed lymphadenopathy on baseline posttreatment PET/CT performed 8–12 weeks after therapy has an NPV of 90–100% [25]. Therefore, negative results of PET/CT performed 12 weeks after treatment are highly reassuring, allowing a patient to forgo salvage treatment. PET/CT performed earlier than 12 weeks after treatment yields a larger number of false-positive results due to inflammation or tumor that is slow to respond to treatment. However, specificity is as high as 100% on PET/CT performed 12–16 weeks after therapy [25] (Fig. 3). Establishing a posttreatment anatomic baseline by use of CT or MRI is also useful given that surgery and radiation significantly distort the head and neck anatomy. In summary, the literature and guidelines support performing initial baseline posttreatment imaging approximately 12 weeks after completion of therapy, ideally by contrast-enhanced PET/CT, to assess therapy response at the primary site and at the nodal basin and to establish a baseline for future comparison.

The role of surveillance imaging beyond the baseline posttreatment examination of asymptomatic patients is less clear, with a paucity of literature showing a survival advantage or other clear benefit [26–29]. However, 79% of surveyed head and neck surgeons acknowledged performing imaging surveillance in asymptomatic patients [27], and one study showed clinically occult recurrences in more than one-third of patients, 80% of which occurred later than 6 months after treatment [28] (Fig. 4). Given the combination of high recurrence rates and the difficulty in assessing recurrences,

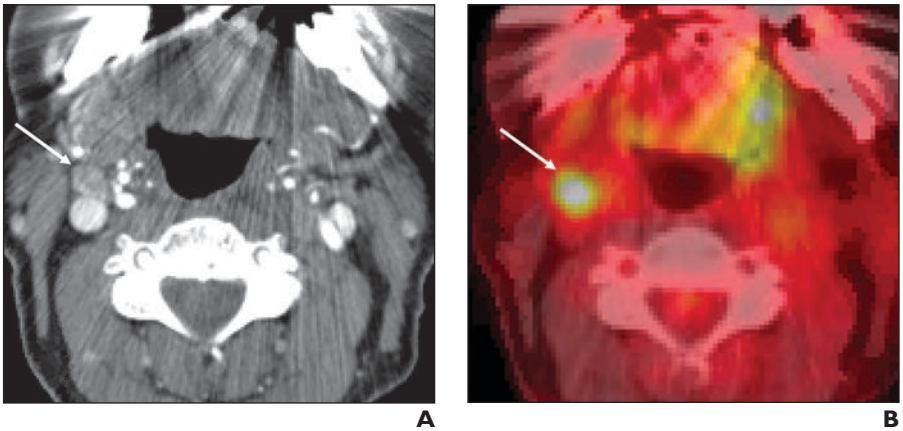

Fig. 4—46-year-old woman with history of T2N1 human papillomavirus–positive squamous cell carcinoma of left tonsil with left neck nodal metastasis, treated with chemoradiation therapy.
A, Axial contrast-enhanced CT image from posttreatment surveillance PET/CT shows pathologic-appearing level II lymph node in contralateral right neck (*arrow*).
B, Axial PET image corresponding to image in **A** shows positive FDG uptake in this node (*arrow*). Patient was asymptomatic, and no lymphadenopathy was detected on clinical examination. PET/CT examination is consistent with Neck Imaging Reporting and Data System category 3 findings in neck (high suspicion for recurrence; biopsy recommended). Patient underwent salvage neck dissection and remained disease free after 18 months of follow-up.

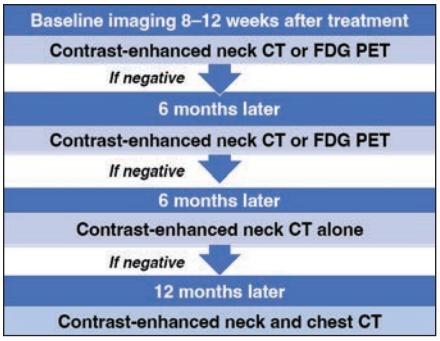

Fig. 5—Algorithm for surveillance imaging after treatment of head and neck cancer, based on Neck Imaging Reporting and Data System. Algorithm entails baseline contrast-enhanced FDG PET/CT performed 8–12 weeks after treatment, followed by imaging performed at 6- to 12-month intervals for 24 months in absence of recurrence. Additional imaging would be performed if surveillance examinations show suspicious findings.

some institutions perform routine imaging surveillance for advanced HNSCC for the first 2–3 years after treatment. Contrast-enhanced CT is generally the primary method used for surveillance cross-sectional imaging of the head and neck. However, MRI may be used for surveillance of sinonasal, nasopharyngeal, orbital, or advanced parotid malignancies [30], given the superiority of MRI for evaluating tumors adjacent to the skull base with the potential for intracranial, intraorbital, or perineural tumor spread. Advanced HNSCC may be associated with pulmonary metastases or primary lung cancers. Therefore, in patients with a history of smoking, annual lung screening by chest CT or PET/CT should be considered for at least the first 2 years, if not for 5 or 10 years [31]. Regardless of the protocol adopted, surveillance imaging should be standardized with respect to technical parameters to facilitate reliable comparison between serial examinations.

Once an imaging surveillance protocol is adopted, the surveillance imaging should be evaluated using a standardized interpretation approach and reporting template such as the American College of Radiology Neck Imaging Reporting and Data System (NI-RADS). NI-RADS was developed to standardize the approach to, reporting of, and management recommendations for HNSCC surveillance imaging. In a 2018 report, the NI-RADS committee proposed a standardized surveillance imaging algorithm, recommending baseline imaging 8–12 weeks after completion of definitive therapy [29] (Fig. 5). If this initial study is negative, then contrast-enhanced neck CT or contrast-enhanced PET/CT should be performed 6 months later. If that first follow-up test is negative, then contrast-enhanced CT of the neck alone is performed 6 months later. If that second follow-up test is negative, then contrast-enhanced CT of the neck and chest is performed 12 months later. The NI-RADS reporting templates provide a lexicon for describing the primary site and the regional nodal basin and also incorporate a level of suspicion for recurrence at each site that is linked to management recommendations [29]. NI-RADS has been shown to improve reporting consistency and communication through actionable reports that help guide clinical management [29, 32]. Studies have also shown reasonable interreader agreement and excellent discriminatory power among the NI-RADS assessment categories [33–36]. The specific categories and linked management recommendations are described in detail in the 2018 report [29] (Table 3), and additional articles outline how to use NI-RADS to help predict residual or recurrent tumor [37, 38].

TABLE 3: NI-RADS Category Descriptors, Imaging Findings, and Management

Category	Category	Imaging Findings	Management
Incomplete	0	▪ New baseline study without any prior imaging available *and* knowledge that prior imaging exists and will become available as comparison*	Assign score in addendum after prior imaging examinations become available
No evidence of recurrence	1	▪ Expected posttreatment changes ▪ Non-mass-like distortion of soft tissues ▪ Low-density "mucoid" mucosal edema ▪ No abnormal FDG uptake ▪ Diffuse linear mucosal enhancement after radiation	Routine surveillance
Low suspicion	2a	▪ Focal mucosal enhancement, but not mass-like ▪ Focal mild to moderate mucosal FDG uptake	Direct visual inspection
	2b	▪ Deep, ill-defined soft tissue, not discrete ▪ Little to no differential enhancement ▪ Mild or moderate FDG uptake	Short-interval follow-up (3 months), repeat PET
High suspicion	3	▪ New or enlarging primary mass or lymph node ▪ Discrete nodule or mass with differential enhancement ▪ Intense focal FDG uptake	Image guided or clinical biopsy
Definitive recurrence	4	▪ Pathologically proven or definite radiologic and clinical progression	Clinical management

Note—NI-RADS = Neck Imaging Reporting and Data Systems. (Reprinted from *Journal of the American College of Radiology*, 15(8), Aiken AH, Rath TJ, Anzai Y, Branstetter BF, Hoang JK, Wiggins RH, Juliano AF, Glastonbury C, Phillips CD, Brown R, Hudgins PA, ACR Neck Imaging Reporting and Data Systems (NI-RADS): A White Paper of the ACR NI-RADS Committee, 1097–1108, Copyright 2018, with permission from American College of Radiology. https://www.sciencedirect.com/journal/journal-of-the-american-college-of-radiology)

*Morphologically abnormal features that are definitive = new necrosis or gross extra nodal extension as evidenced by invasion of adjacent structures.

The approach to imaging surveillance is anticipated to evolve in the era of personalized medicine. The detection of circulating tumor biomarkers, such as plasma HPV or Epstein-Barr virus (EBV) DNA, in the serum of patients treated for viral-associated oropharyngeal or nasopharyngeal carcinoma appears to be extremely sensitive for detection of recurrent disease, with a PPV of up to 94% [21, 39]. These biomarkers will likely guide posttreatment imaging strategies, possibly even replacing imaging surveillance in asymptomatic patients.

How Does Clinical and Immunohistochemical Information Influence the Imaging Evaluation of Patients With NCUP?

NCUP, representing 3% of new cases of head and neck cancer [40], is defined as the clinical presentation of metastatic cervical nodal disease without an obvious primary tumor by both clinical examination and initial imaging evaluation. This designation is frequently transient, as subsequent workup usually leads to the identification of a cutaneous or mucosal head and neck primary tumor. NCUP typically involves level I, II, III, or VA lymph nodes. In comparison, isolated supraclavicular lymphadenopathy (i.e., levels IV and VB) usually arises from primary disease in the thyroid gland or an infraclavicular organ. Some patients with NCUP are found to have lymphoma or other noncarcinoma metastatic lesions [41].

Clinical and Imaging Evaluation

The initial workup of NCUP involves a comprehensive clinical examination, office-based endoscopy, fine-needle aspiration (FNA) of the presenting neck lymph node, and cross-sectional imaging. Operative endoscopy with directed biopsies and palatine and/or lingual tonsillectomy are often required for definitive diagnosis. Both the clinical and the imaging workup vary widely, on the basis of institutional practice as well as local health insurance and pricing patterns. Further research, including cost-effectiveness analyses, are needed to guide optimal evaluation strategies, including choice of imaging modality.

The HPV or EBV status of the FNA sample acquired from the pathologic lymph node provides critical initial information, as more than 90% of cases of NCUP are HPV related [41, 42]. HPV-related NCUP usually has a primary tumor located within the oropharynx, with 43% found within the palatine tonsils and 39% in the lingual tonsils or base of the tongue [43]. After oropharyngeal tumors, the next most common occult primary tumor presenting as NCUP is EBV-related nasopharyngeal carcinoma. EBV-related nasopharyngeal carcinoma is diagnosed by EBV-related RNA testing by in situ hybridization; testing should be performed when *p16* status is negative [44]. Primary tumor sites in patients with EBV-positive metastatic cervical lymphadenopathy include the nasopharynx (51.7%), salivary gland (24.5%), lung (7.8%), and liver (0.4%) [45]. EBV-positive primary salivary gland tumors metastasize mostly to level I and II lymph nodes, whereas EBV-positive primary lung or liver tumors usually metastasize to level IV lymph nodes.

Although *p16*-positive status is highly correlated with HPV infection in HNSCC, *p16* expression is not limited to HPV-positive tumors, such that *p16* is an imperfect surrogate marker for HPV-related head and neck neoplasia. A *p16*-positive neck mass unrelated to HPV may arise from a cutaneous or pulmonary primary tumor. This differentiation requires additional testing to directly evaluate for viral genetic material to support an oropharyngeal versus nonoropharyngeal site of origin. In such patients, chest CT or whole-body FDG PET/CT is useful to identify a lung primary, especially in the setting of a metastatic lymph node in the low neck (levels IV and V) [46]. If an unknown cutaneous primary site is suspected, then DNA damage evaluation can be performed on the nodal FNA sample. Next-generation sequencing can identify ultraviolet light DNA damage signatures consisting of a higher number of C-to-T substitution–type somatic mutations that are specific for skin cancer [47].

Established guidelines for selecting imaging modalities to identify an occult primary site are lacking, and this assessment is currently accomplished by any combination of contrast-enhanced CT, MRI, or FDG PET. Occult HPV-related primary oropharyngeal SCC may be extremely small or located within the tonsillar crypts, thus being impossible to identify on direct visual inspection or on palpation. However, such tumors may be visible on imaging even when not apparent on clinical examination. Imaging findings include subtle asymmetry in size, irregularity (especially along the deep margins of the tonsils, adjacent glossotonsillar sulcus, and base of tongue), or variability in internal architecture (e.g., different signal intensity, attenuation, or enhancement vs normal tissue). Imaging interpretation requires careful evaluation of the shape, margins, and enhancement pattern of the lingual and palatine tonsils. On MRI, the lesion may only be identified on DWI given background tissue suppression that may increase the conspicuity of cellular primary tumor [48] (Fig. 6). The lesion may also be identified only by contrast-enhanced FDG PET/CT (Fig. 7). Although FDG PET has high sensitivity (73.1%) and NPV (68.9%) for detecting the primary site in NCUP compared with other modalities, it is prone to false positives and false negatives and has limited overall accuracy, especially for small primary tumors [49]. Tonsillectomy, in conjunction with direct laryngoscopy under general anesthesia, identifies primary tumors in a substantial percentage of patients with negative FDG PET [50]. As false-positive results on FDG PET are common after tonsillar manipulation or palpation or when performed after a prior intervention, such imaging should preferably be performed before tissue sampling. A common source of false-negative results on FDG PET is obscuration of small oropharyngeal primary tumors by physiologic uptake in the normal lingual or palatine tonsillar lymphoid tissue; detection of such tumors may require increasing image contrast by narrowing the image window settings [49]. Other common sources of false-negative results on FDG PET include dental hardware–related artifacts.

Staging and Treatment Overview of NCUP

The 8th edition of the AJCC staging manual identifies three distinct staging systems for NCUP. Those associated with the *p16*-positive or HPV pathway follow the staging system for NCUP of oropharyngeal origin, those associated with the EBV pathway follow the staging system for NCUP of nasopharyngeal origin, and those with both *p16*-negative and EBV-negative status are staged using the generic N category. These three approaches to staging primary T0 tumors reflect the distinct prognostic features in each setting and are described in chapters 10, 9, and 6, respectively, of the AJCC staging manual [51]. Key features in such nodal

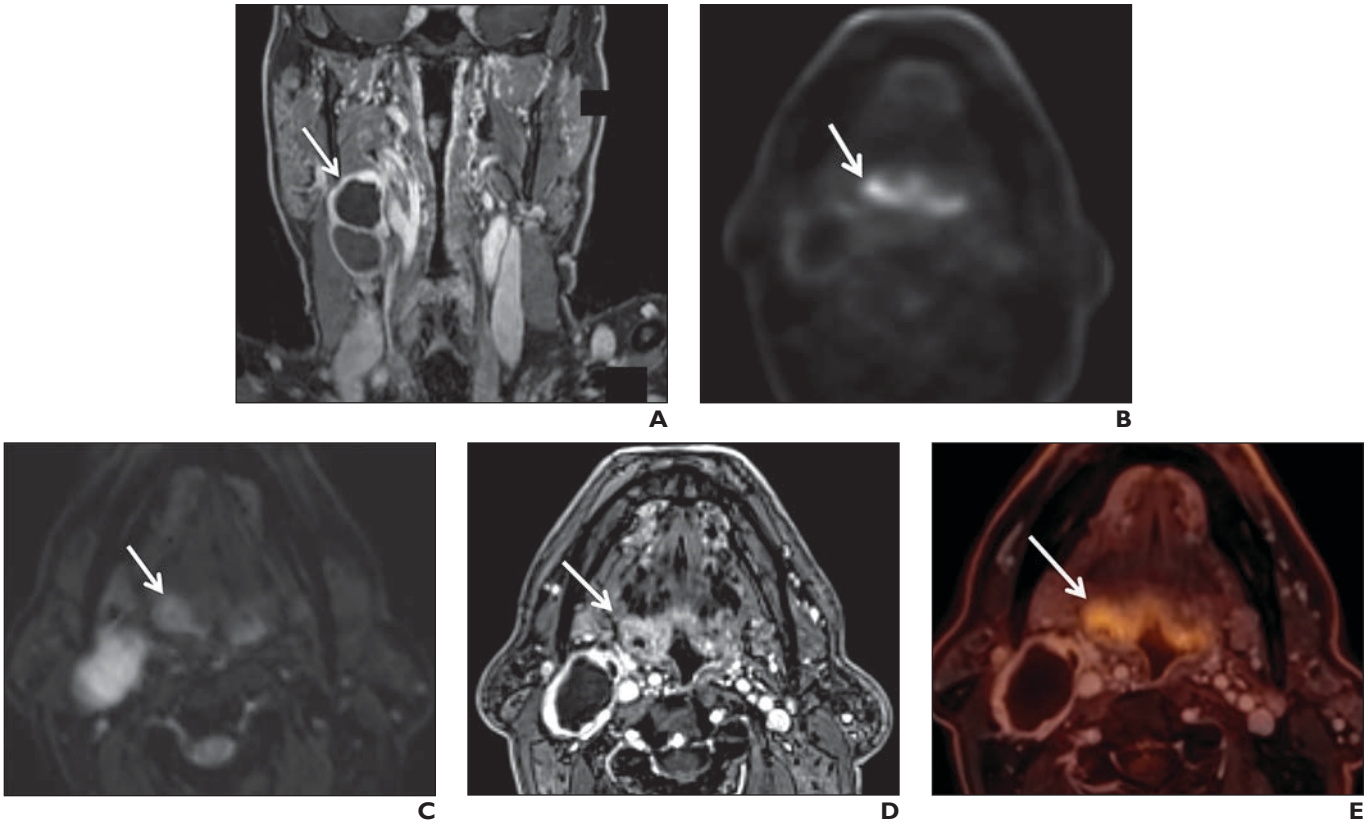

Fig. 6—32-year-old man with squamous cell carcinoma of right base of tongue presenting as right neck carcinoma of unknown primary (NCUP).
A, Coronal contrast-enhanced MR image shows right level 2A cystic nodal lesion (*arrow*). No obvious primary lesion was identified on clinical examination, consistent with NCUP. Right neck nodal lesion underwent ultrasound-guided fine-needle aspiration, which showed *p16*-positive tissue. Patient subsequently underwent hybrid FDG PET/MRI.
B, Axial DW image from PET/MRI examination shows hyperintensity of primary tumor at right base of tongue (*arrow*).
C, Additional axial DW image from PET/MRI examination shows hyperintensity of right level 2A nodal mass (*arrow*). Primary tumor and metastatic node are more conspicuous in comparison with hypointense background.
D, Axial contrast-enhanced MR image from PET/MRI shows primary tumor of right base of tongue (*arrow*).
E, Corresponding fused PET/MR image shows hypermetabolic focus in right base of tongue (*arrow*), consistent with site of primary tumor.

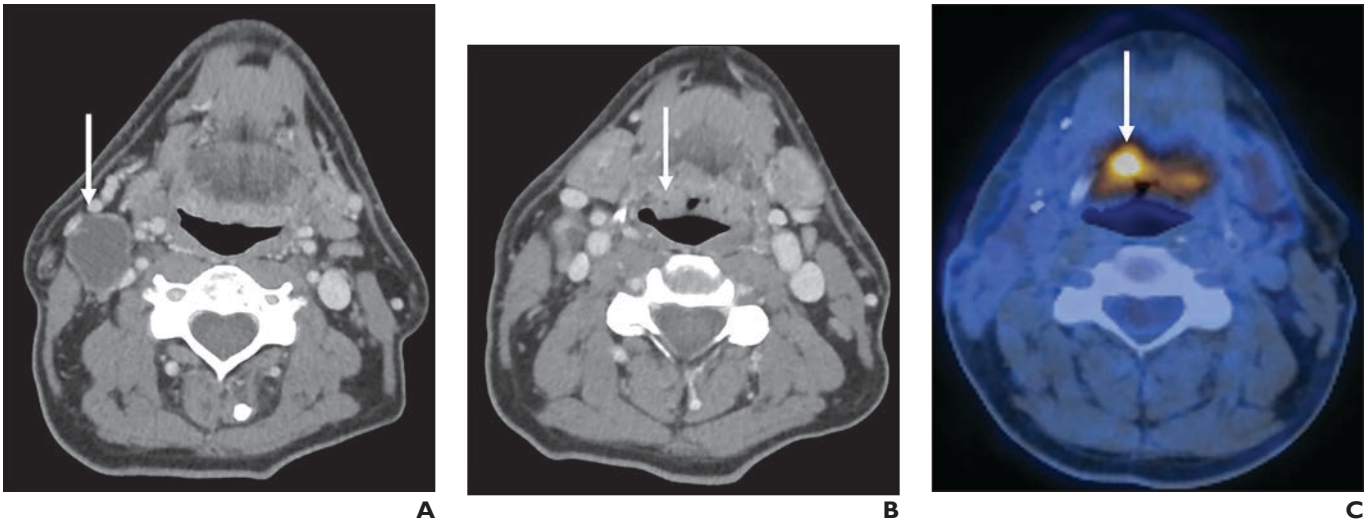

Fig. 7—56-year-old man with *p16* human papillomavirus–positive squamous cell carcinoma of right base of tongue.
A, Axial contrast-enhanced CT image shows right level 2A cystic nodal lesion (*arrow*). Lesion shows *p16* human papillomavirus–positive tissue on fine-needle aspiration. No obvious primary lesion was identified, consistent with neck carcinoma of unknown primary.
B, Axial contrast-enhanced CT image from subsequent FDG PET/CT examination shows lesion in right inferior base of tongue (*arrow*), obscured by overlying mucosa.
C, Corresponding fused PET/CT image shows hypermetabolism of lesion (*arrow*), consistent with primary site of tumor.

staging systems include the presence of ipsilateral, contralateral, or bilateral lymph nodes; nodal size (with long-axis cutoffs of 3 and 6 cm); and extranodal extension [52–54].

The two main goals of treatment in NCUP include achieving locoregional control (for nodal disease) and ensuring treatment of the potential primary site tumor. In patients with NCUP, the status of the metastatic lymph node as HPV related, EBV related, or neither determines the approach to treatment of the likely primary site. Treatment of the neck typically includes either upfront surgery followed by radiation therapy with or without chemotherapy or upfront definitive radiotherapy with or without chemotherapy [50]. For patients undergoing upfront neck dissection, a common approach is to concurrently assess for the primary tumor by removing the ipsilateral tonsil and performing intraoperative frozen section analysis, followed by lingual tonsillectomy if the palatine tonsil yields benign pathologic results. If the primary site is identified, resection is performed in the same setting, often through a transoral robotic approach [55].

What Is the Current Role of Simultaneous PET/MRI in Head and Neck Cancer?

PET/MRI systems attempt to leverage the benefits of both the metabolic information derived from PET and the superior soft-tissue contrast and functional imaging capabilities of MRI. Modern, fully integrated PET/MRI systems capable of simultaneous PET and MRI acquisition have been enabled by the development of compact photodetectors insensitive to magnetic fields and readout electronics associated with minimal heat radiation [56]. New PET detector systems have increased sensitivity that permits reduction in administered FDG doses for PET/MRI examinations without compromising image quality [57]. Accurate attenuation correction has been achieved primarily through the use of atlas-based, image segmentation–based, and, more recently, deep learning–based methods [58, 59]. Furthermore, the use of free-breathing motion-robust MRI sequences (e.g., radial VIBE) and zero-TE techniques has enhanced the sensitivity of simultaneous PET/MRI for detection of small and clinically relevant lung nodules [60, 61]. Although a simultaneous PET/MRI examination provides convenience relative to two separate imaging examinations, the small-bore diameters of current PET/MRI systems may be uncomfortable, necessitating tailoring of examinations to minimize scanning time [62]. Numerous neurologic, musculoskeletal, and cardiovascular applications of PET/MRI have been described [56], and large studies have attempted to establish the value of PET/MRI in oncologic imaging [63–65]. Nonetheless, the widespread adoption of the modality has faced substantial operational and economic obstacles.

MRI is used routinely to assess head and neck malignancies and is the primary imaging method used to evaluate for perineural spread and intracranial, orbital, skull base, and prevertebral space invasion [66–68]. FDG PET/CT has established use in HNSCC staging, response assessment, and surveillance [69]. PET/MRI provides the advantages of both modalities in a single imaging session [70, 71], with a substantial reduction in radiation dose compared with performing separate MRI and FDG PET/CT examinations. However, studies describing the use of PET/MRI in HNSCC have had conflicting results [65, 72–74], and the role of the modality in the diagnosis, treatment planning, and follow-up of head and neck cancer remains to be established. Some studies with small patient samples showed no significant differences between MRI, FDG PET/CT, and FDG PET/MRI in the ability to stage local tumor extent or detect tumor recurrence in head and neck cancer [72, 73]. However, other studies suggested that PET/MRI characteristics may help predict overall survival in patients with aerodigestive tract cancer treated with chemoradiation [73] or may be superior to PET/CT in patients with NCUP [74] (Fig. 6). In addition, in a study from 2022, PET/MRI had excellent discriminatory performance for predicting the treatment outcomes of HNSCC using NI-RADS [75]. In another study, simultaneously acquired FDG PET and DWI yielded excellent results for detection and local staging of HNSCC after chemoradiation [76].

Given the promising nature of some of the available studies, larger prospective multicenter trials are warranted to further assess the role of FDG PET/MRI in head and neck cancer [77]. Even if FDG PET/MRI is shown to be clinically useful for head and neck cancer, cost-related issues (e.g., for purchase, maintenance, and reimbursement) also must be considered. Time-efficient protocols (e.g., using single 3D rather than multiplanar 2D MRI acquisitions) that answer targeted clinical questions should be designed. A study from 2020 suggested that GBCA administration had no added benefit for local tumor staging when FDG PET/MRI of the head and neck is performed and thus could potentially be avoided [78]. Finally, practical standardized protocols would need to be developed for FDG PET/MRI to be adopted into widespread clinical practice, including in community settings, for head and neck cancer evaluation.

Consensus Statements

MRI Protocols for Head and Neck Cancer

- MRI for the evaluation of head and neck cancer should routinely include T1-weighted imaging without FS, T2-weighted imaging with FS, and postcontrast T1-weighted imaging with FS. These sequences should all be reviewed in two or three planes, whether obtained through separate multiplanar 2D acquisitions or reconstruction of a single 3D acquisition.
- MRI for the evaluation of head and neck cancer should routinely include T1-weighted imaging without FS, T2-weighted imaging with FS, and postcontrast T1-weighted imaging with FS. These sequences should all be reviewed in two or three planes, whether obtained through separate multiplanar 2D acquisitions or reconstruction of a single 3D acquisition.

Surveillance Imaging in Head and Neck Squamous Cell Cancer

- The available evidence supports routinely acquiring a baseline surveillance imaging examination within the first 6 months after treatment. The most widely accepted practice is to perform a contrast-enhanced PET/CT at 8–12 weeks after completion of therapy.
- The ACR NI-RADS interpretation approach and reporting templates should be used for surveillance imag-

ing examinations. Use of NI-RADS improves the consistency of reporting and communication, guides clinical management, and contributes to a repository of data to aid in future outcomes-based research examinations. Use of NI-RADS improves the consistency of reporting and communication, guides clinical management, and contributes to a repository of data to aid in future outcomes-based research.

- The ACR NI-RADS interpretation approach and reporting templates should be used for surveillance imaging examinations. Use of NI-RADS improves the consistency of reporting and communication, guides clinical management, and contributes to a repository of data to aid in future outcomes-based research.

Imaging in NCUP

- Imaging evaluation in NCUP must consider *p16* and HPV status (typically positive in oropharyngeal tumors) as well as EBV status (typically positive in nasopharyngeal tumors). These markers guide the radiologist in identification of the primary site. Most cases of NCUP are due to *p16*-positive HPV-associated primary tumors of the oropharynx, thus requiring meticulous evaluation of this region on imaging.
- For cases of NCUP that are both HPV and EBV negative, primary sites involving the skin, mucosal surfaces outside of the nasopharynx and oropharynx, and infraclavicular organs should be considered.

Simultaneous PET/MRI in Head and Neck Squamous Cell Cancer

- The role of simultaneous PET/MRI in head and neck cancer remains undefined. Studies suggest that PET/MRI may improve assessment of local tumor extent compared with PET/CT. However, large prospective multicenter studies are needed to establish the modality's value.

Provenance and review: Solicited; externally peer reviewed.

References

1. Taberna M, Mena M, Pavón MA, Alemany L, Gillison ML, Mesía R. Human papillomavirus-related oropharyngeal cancer. *Ann Oncol* 2017; 28:2386–2398
2. Economopoulou P, Kotsantis I, Psyrri A. De-escalating strategies in HPV-associated head and neck squamous cell carcinoma. *Viruses* 2021; 13:1787
3. Junn JC, Soderlund KA, Glastonbury CM. Imaging of head and neck cancer with CT, MRI, and US. *Semin Nucl Med* 2021; 51:3–12
4. Vishwanath V, Jafarieh S, Rembielak A. The role of imaging in head and neck cancer: an overview of different imaging modalities in primary diagnosis and staging of the disease. *J Contemp Brachytherapy* 2020; 12:512–518
5. Touska P, Connor SEJ. Recent advances in MRI of the head and neck, skull base and cranial nerves: new and evolving sequences, analyses and clinical applications. *Br J Radiol* 2019; 92:20190513
6. Ross MR, Schomer DF, Chappell P, Enzmann DR. MR imaging of head and neck tumors: comparison of T1-weighted contrast-enhanced fat-suppressed images with conventional T2-weighted and fast spin-echo T2-weighted images. *AJR* 1994; 163:173–178
7. Widmann G, Henninger B, Kremser C, Jaschke W. MRI sequences in head & neck radiology: state of the art. *Rofo* 2017; 189:413–422
8. El Beltagi AH, Elsotouhy AH, Own AM, Abdelfattah W, Nair K, Vattoth S. Functional magnetic resonance imaging of head and neck cancer: performance and potential. *Neuroradiol J* 2019; 32:36–52
9. Chawla S, Kim S, Wang S, Poptani H. Diffusion-weighted imaging in head and neck cancers. *Future Oncol* 2009; 5:959–975
10. Surov A, Meyer HJ, Wienke A. Apparent diffusion coefficient for distinguishing between malignant and benign lesions in the head and neck region: a systematic review and meta-analysis. *Front Oncol* 2020; 9:1362
11. Connolly M, Srinivasan A. Diffusion-weighted imaging in head and neck cancer: technique, limitations, and applications. *Magn Reson Imaging Clin N Am* 2018; 26:121–133
12. Verhappen MH, Pouwels PJW, Ljumanovic R, et al. Diffusion-weighted MR imaging in head and neck cancer: comparison between half-Fourier acquired single-shot turbo spin-echo and EPI techniques. *AJNR* 2012; 33:1239–1246
12. Abdel Razek AAK, Gaballa G, Ashamalla G, Alashry MS, Nada N. Dynamic susceptibility contrast perfusion-weighted magnetic resonance imaging and diffusion-weighted magnetic resonance imaging in differentiating recurrent head and neck cancer from postradiation changes. *J Comput Assist Tomogr* 2015; 39:849–854
13. Furukawa M, Parvathaneni U, Maravilla K, Richards TL, Anzai Y. Dynamic contrast-enhanced MR perfusion imaging of head and neck tumors at 3 Tesla. *Head Neck* 2013; 35:923–929
14. Kabadi SJ, Fatterpekar GM, Anzai Y, Mogen J, Hagiwara M, Patel SH. Dynamic contrast-enhanced MR imaging in head and neck cancer. *Magn Reson Imaging Clin N Am* 2018; 26:135–149
15. Gaddikeri S, Gaddikeri RS, Tailor T, Anzai Y. Dynamic contrast-enhanced MR imaging in head and neck cancer: techniques and clinical applications. *AJNR* 2016; 37:588–595
16. Jansen JFA, Parra C, Lu Y, Shukla-Dave A. Evaluation of head and neck tumors with functional MR imaging. *Magn Reson Imaging Clin N Am* 2016; 24:123–133
17. Bruixola G, Remacha E, Jiménez-Pastor A, et al. Radiomics and radiogenomics in head and neck squamous cell carcinoma: potential contribution to patient management and challenges. *Cancer Treat Rev* 2021; 99:102263
18. Carla C, Daris F, Cecilia B, Francesca B, Francesca C, Paolo F. Angiogenesis in head and neck cancer: a review of the literature. *J Oncol* 2012; 2012:358472
19. Martín-Noguerol T, Kirsch CFE, Montesinos P, Luna A. Arterial spin labeling for head and neck lesion assessment: technical adjustments and clinical applications. *Neuroradiology* 2021; 63:1969–1983
20. Chang JH, Wu CC, Yuan KSP, Wu ATH, Wu SY. Locoregionally recurrent head and neck squamous cell carcinoma: incidence, survival, prognostic factors, and treatment outcomes. *Oncotarget* 2017; 8:55600–55612
21. Janopaul-Naylor JR, Aiken AH, Saba NF, El-Deiry M, Kaka AS, Stokes WA. To scan or not to scan: the dilemma of posttreatment imaging surveillance of head and neck cancer. *Pract Radiat Oncol* 2022 12:210–214
22. Mehanna H, Wong WL, McConkey CC, et al.; PET-NECK Trial Management Group. PET-CT surveillance versus neck dissection in advanced head and neck cancer. *N Engl J Med* 2016; 374:1444–1454
23. Branstetter BF 4th, Blodgett TM, Zimmer LA, et al. Head and neck malignancy: is PET/CT more accurate than PET or CT alone? *Radiology* 2005; 235:580–586
24. Beswick DM, Gooding WE, Johnson JT, Branstetter BF 4th. Temporal patterns of head and neck squamous cell carcinoma recurrence with positron-emission tomography/computed tomography monitoring. *Laryngo-*

scope 2012; 122:1512–1517
25. Bar-Ad V, Mishra M, Ohri N, Intenzo C. Positron emission tomography for neck evaluation following definitive treatment with chemoradiotherapy for locoregionally advanced head and neck squamous cell carcinoma. *Rev Recent Clin Trials* 2012; 7:36–41
26. Ng SP, Pollard C 3rd, Berends J, et al. Usefulness of surveillance imaging in patients with head and neck cancer who are treated with definitive radiotherapy. *Cancer* 2019; 125:1823–1829
27. Roman BR, Patel SG, Wang MB, et al. Guideline familiarity predicts variation in self-reported use of routine surveillance PET/CT by physicians who treat head and neck cancer. *J Natl Compr Canc Netw* 2015; 13:69–77
28. Gore A, Baugnon K, Beitler J, et al. Posttreatment imaging in patients with head and neck cancer without clinical evidence of recurrence: should surveillance imaging extend beyond 6 months? *AJNR* 2020; 41:1238–1244
29. Aiken AH, Rath TJ, Anzai Y, et al. ACR Neck Imaging Reporting and Data Systems (NI-RADS): a white paper of the ACR NI-RADS Committee. *J Am Coll Radiol* 2018; 15:1097–1108
30. Zuchowski C, Kemme J, Aiken AH, Baugnon KL, Abdel Razek AAK, Wu X. Posttreatment magnetic resonance imaging surveillance of head and neck cancers. *Magn Reson Imaging Clin N Am* 2022; 30:109–120
31. Alnefaie M, Alamri A, Saeedi A, et al. Pulmonary screening practices of otolaryngology–head and neck surgeons across Saudi Arabia in the posttreatment surveillance of squamous cell carcinoma: cross-sectional survey study. *Interact J Med Res* 2022; 11:e24592
32. Bunch PM, Meegalla NT, Abualruz AR, et al. Initial referring physician and radiologist experience with Neck Imaging Reporting and Data System. *Laryngoscope* 2022; 132:349–355
33. Krieger DA, Hudgins PA, Nayak GK, et al. Initial performance of NI-RADS to predict residual or recurrent head and neck squamous cell carcinoma. *AJNR* 2017; 38:1193–1199
34. Dinkelborg P, Ro SR, Shnayien S, et al. Retrospective evaluation of NI-RADS for detecting postsurgical recurrence of oral squamous cell carcinoma on surveillance CT or MRI. *AJR* 2021; 217:198–206
35. Abdelaziz TT, Abdel Razk AAK, Ashour MMM, Abdelrahman AS. Interreader reproducibility of the Neck Imaging Reporting and Data System (NI-RADS) lexicon for the detection of residual/recurrent disease in treated head and neck squamous cell carcinoma (HNSCC). *Cancer Imaging* 2020; 20:61
36. Hsu D, Rath TJ, Branstetter BF, et al. Interrater reliability of NI-RADS on posttreatment PET/contrast-enhanced CT scans in head and neck squamous cell carcinoma. *Radiol Imaging Cancer* 2021; 3:e200131
37. Strauss SB, Aiken AH, Lantos JE, Phillips CD. Best practices: application of NI-RADS for posttreatment surveillance imaging of head and neck cancer. *AJR* 2021; 216:1438–1451
38. Baugnon KL. NI-RADS to predict residual or recurrent head and neck squamous cell carcinoma. *Neuroimaging Clin N Am* 2022; 32:1–18
39. Haring CT, Dermody SM, Yalamanchi P, et al. The future of circulating tumor DNA as a biomarker in HPV related oropharyngeal squamous cell carcinoma. *Oral Oncol* 2022; 126:105776
40. Strojan P, Ferlito A, Langendijk JA, et al. Contemporary management of lymph node metastases from an unknown primary to the neck: II. A review of therapeutic options. *Head Neck* 2013; 35:286–293
41. Gupta RK, Naran S, Lallu S, Fauck R. The diagnostic value of fine needle aspiration cytology (FNAC) in the assessment of palpable supraclavicular lymph nodes: a study of 218 cases. *Cytopathology* 2003; 14:201–207
42. Motz K, Qualliotine JR, Rettig E, Richmon JD, Eisele DW, Fakhry C. Changes in unknown primary squamous cell carcinoma of the head and neck at initial presentation in the era of human papillomavirus. *JAMA Otolaryngol Head Neck Surg* 2016; 142:223–228
43. Keller LM, Galloway TJ, Holdbrook T, et al. p16 Status, pathologic and clinical characteristics, biomolecular signature, and long-term outcomes in head and neck squamous cell carcinomas of unknown primary. *Head Neck* 2014; 36:1677–1684
44. Lee WY, Hsiao JR, Jin YT, Tsai ST. Epstein-Barr virus detection in neck metastases by in-situ hybridization in fine-needle aspiration cytologic studies: an aid for differentiating the primary site. *Head Neck* 2000; 22:336–340
45. Luo WJ, Feng YF, Guo R, et al. Patterns of EBV-positive cervical lymph node involvement in head and neck cancer and implications for the management of nasopharyngeal carcinoma T0 classification. *Oral Oncol* 2019; 91:7–12
46. Miller FR, Karnad AB, Eng T, Hussey DH, Stan McGuff H, Otto RA. Management of the unknown primary carcinoma: long-term follow-up on a negative PET scan and negative panendoscopy. *Head Neck* 2008; 30:28–34
47. Chan JW, Yeh I, El-Sayed IH, et al. Ultraviolet light-related DNA damage mutation signature distinguishes cutaneous from mucosal or other origin for head and neck squamous cell carcinoma of unknown primary site. *Head Neck* 2019; 41:E82–E85
48. Ravanelli M, Grammatica A, Tononcelli E, et al. Correlation between human papillomavirus status and quantitative MR imaging parameters including diffusion-weighted imaging and texture features in oropharyngeal carcinoma. *AJNR* 2018; 39:1878–1883
49. Sokoya M, Chowdhury F, Kadakia S, Ducic Y. Combination of panendoscopy and positron emission tomography/computed tomography increases detection of unknown primary head and neck carcinoma. *Laryngoscope* 2018; 128:2573–2575
50. Maghami E, Ismaila N, Alvarez A, et al. Diagnosis and management of squamous cell carcinoma of unknown primary in the head and neck: ASCO guideline. *J Clin Oncol* 2020; 38:2570–2596
51. Amin M, Edge S, Greene F, eds. *AJCC cancer staging manual*, 8th ed. Springer-Verlag, 2017
52. Bauer E, Mazul A, Chernock R, et al. Extranodal extension is a strong prognosticator in HPV-positive oropharyngeal squamous cell carcinoma. *Laryngoscope* 2020; 130:939–945
53. Kimura Y, Sumi M, Sakihama N, Tanaka F, Takahashi H, Nakamura T. MR imaging criteria for the prediction of extranodal spread of metastatic cancer in the neck. *AJNR* 2008; 29:1355–1359
54. Patel MR, Hudgins PA, Beitler JJ, et al. Radiographic imaging does not reliably predict macroscopic extranodal extension in human papilloma virus–associated oropharyngeal cancer. *ORL J Otorhinolaryngol Relat Spec* 2018; 80:85–95
55. Graboyes EM, Sinha P, Thorstad WL, Rich JT, Haughey BH. Management of human papillomavirus–related unknown primaries of the head and neck with a transoral surgical approach. *Head Neck* 2015; 37:1603–1611
56. Torigian DA, Zaidi H, Kwee TC, et al. PET/MR imaging: technical aspects and potential clinical applications. *Radiology* 2013; 267:26–44
57. Sekine T, Delso G, Zeimpekis KG, et al. Reduction of ^{18}F-FDG dose in clinical PET/MR imaging by using silicon photomultiplier detectors. *Radiology* 2018; 286:249–259
58. Chen Y, An H. Attenuation correction of PET/MR imaging. *Magn Reson Imaging Clin N Am* 2017; 25:245–255
59. Liu F, Jang H, Kijowski R, Bradshaw T, McMillan AB. Deep learning MR imaging-based attenuation correction for PET/MR imaging. *Radiology* 2018; 286:676–684
60. Chandarana H, Heacock L, Rakheja R, et al. Pulmonary nodules in patients with primary malignancy: comparison of hybrid PET/MR and PET/CT imaging. *Radiology* 2013; 268:874–881
61. Zeng F, Nogami M, Ueno YR, et al. Diagnostic performance of zero-TE lung

MR imaging in FDG PET/MRI for pulmonary malignancies. *Eur Radiol* 2020; 30:4995–5003

62. Kesner AL. The evolution of PET/MR is hindered by our field's reluctance to provide critical evaluation. *J Nucl Med* 2021; 62:462–463
63. Catalano OA, Rosen BR, Sahani DV, et al. Clinical impact of PET/MR imaging in patients with cancer undergoing same-day PET/CT: initial experience in 134 patients—a hypothesis-generating exploratory study. *Radiology* 2013; 269:857–869
64. Mayerhoefer ME, Prosch H, Beer L, et al. PET/MRI versus PET/CT in oncology: a prospective single-center study of 330 examinations focusing on implications for patient management and cost considerations. *Eur J Nucl Med Mol Imaging* 2020; 47:51–60
65. Martin O, Schaarschmidt BM, Kirchner J, et al. PET/MRI versus PET/CT for whole-body staging: results from a single-center observational study on 1,003 sequential examinations. *J Nucl Med* 2020; 61:1131–1136
66. Imre A, Pinar E, Erdoğan N, et al. Prevertebral space invasion in head and neck cancer: negative predictive value of imaging techniques. *Ann Otol Rhinol Laryngol* 2015; 124:378–383
67. Hanna E, Vural E, Prokopakis E, Carrau R, Snyderman C, Weissman J. The sensitivity and specificity of high-resolution imaging in evaluating perineural spread of adenoid cystic carcinoma to the skull base. *Arch Otolaryngol Head Neck Surg* 2007; 133:541–545
68. Turri-Zanoni M, Lambertoni A, Margherini S, et al. Multidisciplinary treatment algorithm for the management of sinonasal cancers with orbital invasion: a retrospective study. *Head Neck* 2019; 41:2777–2788
69. Goel R, Moore W, Sumer B, Khan S, Sher D, Subramaniam RM. Clinical practice in PET/CT for the management of head and neck squamous cell cancer. *AJR* 2017; 209:289–303
70. Davis AJ, Rehmani R, Srinivasan A, Fatterpekar GM. Perfusion and permeability imaging for head and neck cancer: theory, acquisition, postprocessing, and relevance to clinical imaging. *Magn Reson Imaging Clin N Am* 2018; 26:19–35
71. Sher AC, Seghers V, Paldino MJ, et al. Assessment of sequential PET/MRI in comparison with PET/CT of pediatric lymphoma: a prospective study. *AJR* 2016; 206:623–631
72. Schaarschmidt BM, Heusch P, Buchbender C, et al. Locoregional tumour evaluation of squamous cell carcinoma in the head and neck area: a comparison between MRI, PET/CT and integrated PET/MRI. *Eur J Nucl Med Mol Imaging* 2016; 43:92–102
73. Pace L, Nicolai E, Cavaliere C, et al. Prognostic value of ^{18}F-FDG PET/MRI in patients with advanced oropharyngeal and hypopharyngeal squamous cell carcinoma. *Ann Nucl Med* 2021; 35:479–484
74. Ruhlmann V, Ruhlmann M, Bellendorf A, et al. Hybrid imaging for detection of carcinoma of unknown primary: a preliminary comparison trial of whole-body PET/MRI versus PET/CT. *Eur J Radiol* 2016; 85:1941–1947
75. Patel LD, Bridgham K, Ciriello J, et al. PET/MR imaging in evaluating treatment failure of head and neck malignancies: a Neck Imaging Reporting and Data System–based study. *AJNR* 2022; 43:435–441
76. Becker M, Varoquaux AD, Combescure C, et al. Local recurrence of squamous cell carcinoma of the head and neck after radio(chemo)therapy: diagnostic performance of FDG-PET/MRI with diffusion-weighted sequences. *Eur Radiol* 2018; 28:651–663
77. Bailey DL, Pichler BJ, Gückel B, et al. Combined PET/MRI: global warming–summary report of the 6th International Workshop on PET/MRI, March 27–29, 2017, Tübingen, Germany. *Mol Imaging Biol* 2018; 20:4–20
78. Pyatigorskaya N, De Laroche R, Bera G, et al. Are gadolinium-enhanced MR sequences needed in simultaneous ^{18}F-FDG-PET/MRI for tumor delineation in head and neck cancer? *AJNR* 2020; 41:1888–1896